High-Frequency Transformer Isolated AC-DC Converter for Resilient Low Voltage DC Residential Grids

Nelson Santos[1]([✉]), J. Fernando Silva[2], and Vasco Soares[1]

[1] Instituto Superior de Engenharia de Lisboa, INESC-ID,
R. Conselheiro Emídio Navarro, 1959-007 Lisbon, Portugal
{nsantos,vesoares}@deea.isel.ipl.pt
[2] Instituto Superior Técnico, Universidade de Lisboa, INESC-ID,
DEEC, AC Energia, Av. Rovisco Pais, 1049-001 Lisbon, Portugal
fernando.alves@tecnico.ulisboa.pt

Abstract. In a global and growing society, it is necessary to rethink strategies in order to minimize the environmental impact resulting from the progressive increase of energy consumption and the misuse of energy resources. Energy power system converters must be considered as a global way to spare most of the wasted energy. Today, in the power distribution infrastructure, including modern residential buildings, most equipment have power supplies with imbedded AC-DC power converters which may have overall losses as high as 25% regarding the equipment output. Therefore, common DC buses for residential applications are being studied to increase equipment efficiency. This paper presents and designs an AC-DC isolated converter that uses a full-bridge matrix topology with high-frequency isolation transformer and non-electrolytic capacitors to integrate into the future residential buildings DC bus, presenting a reliable alternative to AC power. Non-linear control techniques (sliding mode control and backstepping control) are employed to guarantee stability and disturbance robustness to the output DC low voltage, while enforcing sinusoidal input AC current and power factor correction. Control strategies are described and simulation results are presented and discussed.

Keywords: AC-DC converter · High-frequency transformer
Sliding mode control · Backstepping control · DC residential grids
Smart-grids

1 Introduction

In the last years there is a big motivation to electrical energy generation in a decentralized way, using clean energy resources, like solar and wind. The local generation and consumption would avoid transport losses, improving the affordability of electrical networks. However, the inter-connection of sources, like DC (solar) and AC (wind), with different voltage levels and waveforms, implies their adaptation through electronic power converters and their use in micro-grids has to follow well defined characteristics.

Main electric networks will continue to use AC voltages for compatibility reasons and easy voltage level transformation. However, nowadays most electric loads need DC power obtained via AC-DC switching converter, between the AC input voltage 230 V and the DC output voltage from 5 V to 400 V. Therefore, most actual loads such as lighting systems, small appliances and mobile devices could advantageously be supplied from a common DC network, eliminating the need of the embedded AC-DC converter and sparing its losses.

With the recent progress in the semiconductor technologies a single high efficiency central AC-DC converter could be advantageous in eliminating several less reliable and less efficient AC-DC embedded converters. Even if the DC voltage needs to be customized, a DC-DC converter is simpler and presents higher efficiency than an AC-DC converter. Considering also the High Voltage Direct Current (HVDC) technology DC buses are currently an alternative to AC grids, with better use of resources, both in transmission, distribution and in the final consumer place. These advantages will be emphasized by the integration of electric vehicles, as they require a large amount power to handle the fast charging of batteries. The fast charging process may benefit from the DC grid due to the simplicity and efficiency of DC-DC converters compared to the typical AC-DC. Moreover, in DC networks there is no reactive power compensation, no need to synchronize generators for the network frequency, no skin effect and easier power failure mitigation when combined with energy storage systems [1]. On the other hand, DC networks are not directly connectable to electric machines, such as transformers and motors demanding the use of switching converters (at least diode bridge rectifiers for doubly fed induction motors driven with 3 phase inverters). Additionally, it is necessary to adapt the handling equipment including equipment and people protections, while needing an efficient isolated AC-DC converter to link with the mains network.

A characteristic of a DC micro-grid is its voltage level. This level must be selected taking into account the type and the power required by connecting loads. Recently, consensus exists in benefits of use the level around 400 Vdc to cover different types of loads, a value advocated by associations of equipment producers, which may possibly be adopted in the new regulations for the residential and commercial DC distribution networks. For example, the Emerge Alliance's [2], standards recommends 24 Vdc for occupied Space standard (low power appliances, lighting, typically in bedrooms and living rooms, guaranteed safety and efficiently at lower voltage) and 380 Vdc for Data and Telecom Center standard (high power loads, kitchen appliances, air conditioning systems for residential air conditioning and electric vehicles). Values in the order of 48 Vdc, 120 Vdc and 230 Vdc have also been considered [3].

Also within the low voltage level, the USB 3.1 standard must be considered [4], with 3 levels of voltage 5 V, 12 V and 20 V and a maximum current of 5 A, being able to feed loads up to 100 W at the voltage of 20 V. There is a growing trend of using devices with USB connector type-C, such as mobile phones, tablets, laptops and other small devices like heaters, blenders and monitors, lighting, already available in the current market. Socially it is a type of system so well accepted that USB wall-sockets are being installed in private houses and offices buildings.

In this framework, the research question is how to implement the concept of AC-DC power converters with galvanic insulation, but without the use of intermediate electrolytic capacitor DC buses, to provide energy to a DC micro-grid.

This paper propose the use of a single-phase AC-DC power converter, using high frequency transformer isolation, to interconnect the AC power distribution grid network at unity power factor and to supply a DC micro-grid for residential or commercial complex use, with the target of reducing losses, cost and footprint, ensuring required quality parameters for suppliers and consumers.

2 Contribution to Resilient Systems

In an increasingly competitive society focused on improving systems efficiency [5], optimizing stability, security and robustness, smart grids play an important role in the community to help achieve these goals. The infrastructure improvement can happen as long as stakeholders have an open mind to change the way energy is used. To ensure the best operating conditions for producers and consumers, human consumption behaviors must be supervised in order to collect all available information to make the best management choice in a way that can decide and adapt all stakeholders for get energy efficiency and a resilient system. In general, smart grids might quickly adapt to new conditions, which may not be initially foreseen, and thus require a natural and sustainable human action.

In this paper we present an AC-DC converter, without electrolytic capacitors, as a solution or an integral part in the conversion of energy for a smart micro grid DC network, introducing a safe and resilient alternative to the existing AC network. This converter can be applied to network distribution or micro-networks in residential complexes, buildings, individual homes and commercial facilities.

3 AC-DC Power Converter Topology

3.1 Circuit Description

The proposed circuit is a high-frequency transformer isolated AC-DC Converter, as depicted in Fig. 1. Active matrix full-bridge with bidirectional semiconductor technology (SiC MOSFET) with LC filter is used, combining proper control strategy to enforce almost unity power factor and maintaining the source current with mostly the fundamental frequency component. Each S_k switch ($k \in \{1,2,3,4\}$) uses two anti-series connected MOSFET semiconductors to handle bipolar voltages from AC source. At load side this AC-DC converter is composed by a diode full-bride rectifier and LC filter to reduce unwanted harmonics of the high frequency diode rectification of the matrix active bridge and the oscillatory nature of AC single phase power.

The differential equations of the proposed circuit are written in (1), with variables and devices shown in Fig. 1.
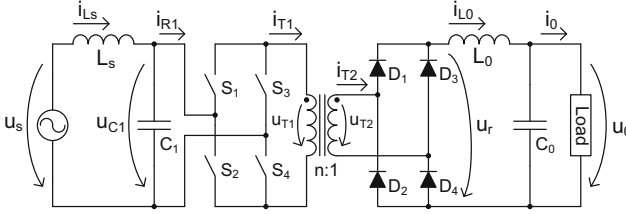
Fig. 1. Proposed high-frequency transformer isolated AC-DC converter.

$$\frac{d}{dt}\begin{bmatrix} u_0 \\ u_{C_1} \\ i_{L_s} \\ i_{L_0} \end{bmatrix} = \begin{bmatrix} 0 & 0 & 0 & 1/C_0 \\ 0 & 0 & 1/C_1 & 0 \\ 0 & -1/L_s & 0 & 0 \\ -1/L_0 & 0 & 0 & 0 \end{bmatrix}\begin{bmatrix} u_0 \\ u_{C_1} \\ i_{L_s} \\ i_{L_0} \end{bmatrix} + \begin{bmatrix} 0 & 0 & 0 & -1/C_0 \\ 0 & 0 & -1/C_1 & 0 \\ 0 & 1/L_s & 0 & 0 \\ 1/L_0 & 0 & 0 & 0 \end{bmatrix}\begin{bmatrix} u_r \\ u_s \\ i_{r_1} \\ i_0 \end{bmatrix} \quad (1)$$

The switches states of S_1, S_2, S_3 and S_4 are represented in (2).

$$\delta(t) = \begin{cases} +1 \rightarrow (S_1, S_4\ ON) \\ 0 \rightarrow (S_1, S_2\ ON\ or\ S_3, S_4\ ON) \\ -1 \rightarrow (S_2, S_3\ ON) \end{cases} \quad (2)$$

3.2 Control

Sliding Mode Internal Voltage Control (u_{C_1}). Considering that, $u_{T_1} = \delta(t)u_{C_1}$ and $i_{r_1} = \delta(t)^2 sgn(u_{C_1})ni_{L_0}$ then, using (1) the phase canonical model for the voltage u_{C_1} is written as (3).

$$\frac{du_{C_1}}{dt} = \frac{1}{C_1}\left(i_{L_s} - \delta(t)^2 sgn(u_{C_1})i_{L_0}/n\right) \quad (3)$$

The first time derivative of u_{C_1} contains the control action $\delta(t)$, thus the strong relative degree of u_{C_1} is 1 [6], and a suitable sliding surface [7–9], can be obtained as a linear combination of the control error $e_{u_{C1}} = u_{C_1}^{ref} - u_{C_1}$ where $u_{C_1}^{ref}$ is the reference value to be tracked by the u_{C_1} voltage. Considering a positive gain k_1, used to bound the semiconductors switching frequency, a suitable sliding surface is $S\left(e_{u_{C_1}}, t\right) = k_1 e_{u_{C_1}} = 0$. The switching strategy is obtained applying the sliding mode stability condition $S\left(e_{u_{C_1}}, t\right)\dot{S}\left(e_{u_{C_1}}, t\right) < 0$. The derivative of $\left(e_{u_{C_1}}, t\right)$, $\dot{S}\left(e_{u_{C_1}}, t\right)$ is:

$$\dot{S}\left(e_{u_{C_1}}, t\right) = k_1\left(\frac{du_{C_1}^{ref}}{dt} - \frac{i_{L_s}}{C_1} + \frac{\delta(t)^2 sgn(u_{C_1})i_{L_0}/n}{C_1}\right) \quad (4)$$

The stability condition is written as (5).

$$
\begin{cases}
if\ S(e_{u_{C_1}}, t) > 0, \text{then}\ \dot{S}(e_{u_{C_1}}, t) < 0 \rightarrow \frac{du_{C1}^{ref}}{dt} - \frac{i_{L_s}}{C_1} + \frac{\delta(t)^2 sgn(u_{C_1}) i_{L_0}/n}{C_1} < 0 \\[2mm]
if\ S(e_{u_{C_1}}, t) < 0, \text{then}\ \dot{S}(e_{u_{C_1}}, t) > 0 \rightarrow \frac{du_{C1}^{ref}}{dt} - \frac{i_{L_s}}{C_1} + \frac{\delta(t)^2 sgn(u_{C_1}) i_{L_0}/n}{C_1} > 0
\end{cases}
\tag{5}
$$

From (5), the sliding mode reaching condition can be obtained as $\frac{\delta(t)^2 sgn(u_{C_1}) i_{L_0}/n}{C_1} > MAX\left(\frac{i_{L_s}}{C_1} - \frac{du_{C_1}^{ref}}{dt}\right)$, Supposing that i_{L_0}/n is high enough to satisfy this reaching condition and the $sgn(u_{C_1}) = sgn(i_{L_s})$, on most situations, the control strategy is written as (6). To impose finite switching frequency, the ripple Δu_{C_1} voltage must be considered and k_1 is selected to ensure stability and fast response.

$$
\begin{cases}
if\ S > 0, \text{then}\ \dot{S} < 0 \rightarrow \begin{cases} u_{C_1} > 0 \rightarrow \delta(t) = 0 \\ u_{C_1} < 0 \rightarrow \delta(t) = \pm 1 \end{cases} \\[4mm]
if\ S < 0, \text{then}\ \dot{S} > 0 \rightarrow \begin{cases} u_{C_1} > 0 \rightarrow \delta(t) = \pm 1 \\ u_{C_1} < 0 \rightarrow \delta(t) = 0 \end{cases}
\end{cases}
\tag{6}
$$

To avoid magnetic saturation of the transformer core an auxiliary control signal, takes advantage of the redundancy presented in (6) to ensure transformer primary voltages with zero average value.

Backstepping Current Control (i_{L_s}). Considering the state variable u_{C_1} whose dynamics can be enforced and using the sub-system (1) the i_{L_s} dynamics can be written as $\frac{di_{L_s}}{dt} = (u_s - u_{C_1})/L_s$. Defining the control objective $e_{i_{L_s}} = 0$, the tracking error is $e_{i_{L_1}} = i_{L_s}^{ref} - i_{L_s}$, and a positive definite Lyapunov function candidate can be selected as $V_1(i_{L_s}, t) = e_{i_{L_s}}^2/2$. From Lyapunov 2$^{\text{nd}}$ method of stability, the time derivative of $V_1\left(e_{i_{L_s}}, t\right)$ must be negative definite for all (i_{L_s}, t), according to $V_1 \dot{V_1} < 0$.

$$
\frac{dV_1}{dt} = e_{i_{L_s}} \frac{de_{i_{L_s}}}{dt} < 0 \Rightarrow e_{i_{L_s}} \frac{de_{i_{L_s}}}{dt} = -k_2 e_{i_{L_s}}^2 \Rightarrow \frac{de_{i_{L_s}}}{dt} = -k_2 e_{i_{L_s}}
\tag{7}
$$

Define a positive constant k_2, selected to impose the time constant of the tracking error converging to zero asymptotically. Solving (7) for $u_{C_1}^{ref}$, the virtual control law [10] is (8).

$$
u_{C1}^{ref} = u_s - k_2 L_s e_{i_{L_s}} - \frac{di_{L_s}^{ref}}{dt} L_s
\tag{8}
$$

The current $i_{L_s}^{ref}$ must be sinusoidal for low THD and in phase with the voltage u_s for near unity power factor, with the amplitude adjusted according to the load consumption. Using a controller, choosing the k_2 to ensure fast response and stability condition, it is intended to control the output voltage u_0 using the input RMS value of input

current i_{L_s}. Assuming the efficiency parameter η, the source power P_s and output power filter P_{L_0}, the input-output power is $P_s\eta = P_{L_0}$ being $U_{s_{rms}}I_{L_{s_{rms}}}\eta = u_0 i_{L_0}$. Using the sub-system (1) Eq. (9) can be written assuming the load output power is P_0.

$$C_0 u_0 \frac{du_0}{dt} = u_0(i_{L_0} - i_0) \Rightarrow \frac{du_0^2}{dt} = \frac{2}{C_0}\left(U_{s_{rms}}I_{L_{s_{rms}}}\eta - P_0\right) \tag{9}$$

Integral Backstepping Voltage Control (u_0). Considering the state variable $I_{L_{s_{rms}}}$ whose dynamics can be enforced. Consider differential Eq. (9) and define the control objective $e_{u_0^2} = 0$. The tracking error being $e_{u_0^2} = u_0^{ref^2} - u_0^2$, add the integral of the tracking error $e_1 = \int e_{u_0^2} dt$ to ensure the convergence, in steady-state, due to the non-modelled disturbances and parameter uncertainty [11] (as an example the efficiency of system). Use a positive definite Lyapunov function V_2 that weights (with k_4) the integral to be added to a new Lyapunov function (10).

$$V_2 = \frac{1}{2}k_4 e_1^2 + \frac{\left(e_{u_0^2}\right)^2}{2} \tag{10}$$

The time derivative of V_2 must be negative definite ($\dot{V}_2 = -k_3 e_{u_0^2}$, $k_3 > 0$), thus:

$$\frac{dV_2}{dt} = k_4 e_1 \frac{de_1}{dt} + e_{u_0^2}\frac{de_{u_0^2}}{dt} = -k_3\left(e_{u_0^2}\right)^2 \tag{11}$$

Using the differential Eqs. (9) and (11), it results (12).

$$k_4 e_1 e_{u_0^2} + e_{u_0^2}\left(\frac{du_0^{ref^2}}{dt} - \frac{2}{C_0}\left(U_{s_{rms}}I_{L_{s_{rms}}}\eta - P_0\right)\right) = -k_3\left(e_{u_0^2}\right)^2 \tag{12}$$

Solving (12) for $I_{L_{s_{rms}}}$, the virtual control law is (13).

$$I_{L_{s_{rms}}} = \frac{C_0}{2\eta U_{s_{rms}}}\left(k_4 e_1 + k_3 e_{u_0^2} + \frac{2P_0}{C_0}\right) \tag{13}$$

Making $i_{L_s}^{ref} = \sqrt{2}I_{L_{s_{rms}}}\sin(\omega t)$ concludes the external loop control design, the current being synchronized to main power AC grid with angular frequency ω. Gains k_3 and k_4 have to be fine-tuned in order to obtain a sufficiently slow response to avoid line current distortion.

3.3 Input and Output LC Filter Design

According to the desired maximum switching frequency f_s for the converter, the L_s and C_1 filter input parameters are calculated by considering voltage ripple Δu_{C_1}, the current ripple Δi_{L_s} and the maximum cycle factor D for maximum power condition

$D = u_0 n\sqrt{2}/\eta U_s$, $C_1 = i_{L_s}D/2f_s\Delta u_{C_1}$ and $L_s = \Delta u_{C_1}D/2f_s\Delta i_{L_s}$, [12]. The output filter L_0 and C_0 is chosen to attenuate the harmonic of order two of AC the amplitude voltage component U_{0_A}, due to rectifier bridge. Establishing the target ripples for current Δi_{L_0} and voltage Δu_{C_0}, according to the desired limitation, it can written $L_0 = U_{0_A}/\omega\Delta i_{L_0}$ and $C_0 = \Delta i_{L_0}/2\omega\Delta u_{C_0}$.

4 Simulation Results

The circuit presented in Fig. 1 was simulated using MATLAB/Simulink considering variations of 25% of load nominal power and the simulation contains the semiconductor models, including the effects of switching and losses. For the simulation parameters it is considered $P_0 = 3\,\text{kW}$, $u_0 = 48\,\text{V}$, $n = 2$, $\eta = 95\%$, $f_s = 50\,\text{kHz}$, $\Delta u_{C_1} = 10\%$, $\Delta i_{L_s} = 2\%$, $\Delta u_{C_0} = 8\%$ and $\Delta i_{L_0} = 10\%$. Figure 2(a) presents the current source i_{L_s}, the voltage u_{C_1}, voltage at the transformer u_{T_1} and the voltage u_0.
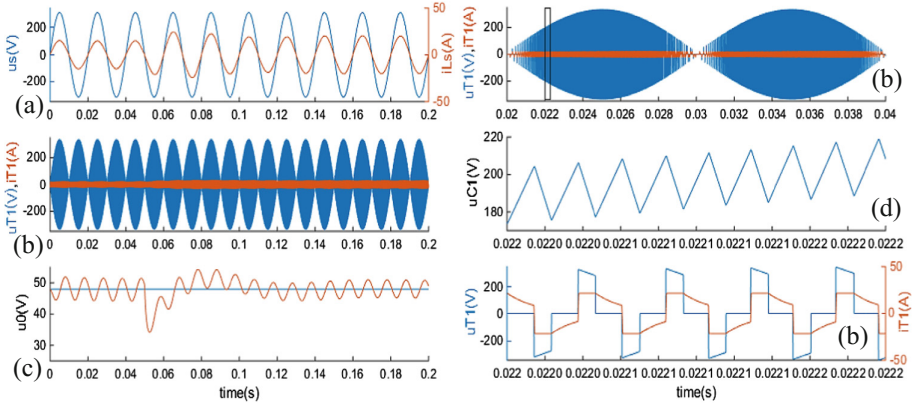
Fig. 2. Temporal evolution; (a) voltage u_s and Current i_{L_s} power source; (b) Transformer voltage u_{T_1} and current i_{T_1}; (c) Output voltage u_0; (d) Voltage u_{C_1}

The current presents maximum THD of 1.8% at nominal load thus improving the power factor, verified in Fig. 2(a). The voltage applied at the transformer primary side (Fig. 2(b)) presents symmetry and zero average value avoiding core saturation and the current presents a rectangular shape with variable frequency and duty cycle, due the control technique, reaching a maximum of 50 kHz. Regarding the output voltage in Fig. 2(c), it presents ripple below 8%. After a load variation of +25% is applied at t=50 ms, the voltage droops 12 V with a recovery time (at 10% of voltage reference) about 60 ms (3 cycles of frequency of main power supply). The Fig. 2(d) represents the voltage ripple at the capacitor C_1 having 10% regarding the source amplitude voltage u_s.

5   Conclusion

This study demonstrates that high-frequency transformer-isolated AC-DC converters can be integrated into future residential buildings with DC bus. Choosing a 48 V DC bus can be a reasonable trade-off regarding human safety and efficiency. This AC-DC isolated converter uses a full-bridge topology with high-frequency isolation transformer working around 40 kHz to improve efficiency and reducing size, and to increase resiliency in energy systems due to the saved energy. This converter combined with energy storage batteries, can further improve resiliency, while reducing the ripple of the output voltage and increasing the response speed to fast request dynamic loads on the DC bus. The non-linear control techniques demonstrate stability and disturbance rejection maintaining sinusoidal input AC current and power factor correction.

References

1. Chauhan, R., Rajpurohit, B., Hebner, R., Singh, S., Gonzalez-Longatt, F.: Voltage standardization of DC distribution system for residential buildings. J. Clean Energy Technol. **4**(3), 167–172 (2016)
2. Public Overview of the Emerge Alliance Data/Telecom Center Standard "Emerge Alliance Advances DC Power to the Desktop", EMerge Alliance, San Ramon, CA, USA (2012)
3. Priyadharshini, G., Nandhini, N.R., Shunmugapriya, S., Ramaprabha, R.: Design and simulation of smart sockets for domestic DC distribution. In: 2017 International Conference on Power and Embedded Drive Control (ICPEDC), Chennai, pp. 426–429 (2017)
4. Shivakumar, A., Normark, B., Welsch, M.: Household DC networks: state of the art and future prospects. InsightE. Rapid Response Energy Brief (2015)
5. Electricity Distribution in the European Union: An Opportunity for Energy Efficiency in Europe. An IEEE European Public Policy Initiative Position Statement. Adopted 27 March 2017. www.ieee.org/about/ieee_europe/eppi_dc_electricitiy_distribution_june_2017.pdf. Accessed 1 Nov 2017
6. Silva, J.F., Pinto, S.F.: Linear and nonlinear control of switching power converters. In: Power Electronics Handbook, Fourth edn., pp. 1141–1220 (2017)
7. Fernando Silva, J.: Sliding mode control of voltage sourced boost-type reversible rectifiers. In: Proceedings of IEEE/ISIE 1997 Conference (ISBN 0-7803-3937-1), Guimarães, Portugal, Julho, vol. 2, pp. 329–334 (1997)
8. Martins, J.F., Pires, A.J., Fernando Silva, J.: A novel and simple current controller for three-phase PWM power inverters. IEEE Trans. Ind. Electr. **45**(5), 802–805 (1998). Special Section on PWM Current Regulation
9. Santos, N., Silva, J.F.A., Santana, J.: Sliding mode control of unified power quality conditioner for 3 phase 4 wire systems. In: Camarinha-Matos, L.M., Barrento, N.S., Mendonça, R. (eds.) DoCEIS 2014. IAICT, vol. 423, pp. 443–450. Springer, Heidelberg (2014). https://doi.org/10.1007/978-3-642-54734-8_49

10. Martin, A.D., Cano, J.M., Silva, F.A., Vazquez, J.R.: Back-stepping control of smart-grid connected distributed photovoltaic power supplies for telecom equipment. IEEE Trans. Energy Convers. **30**(4), 1496–1504 (2015)
11. Tan, Y., Chang, J., Tan, H.: Advanced motion control scheme with integrator backstepping: design and analysis. In: Power Electronics Specialists Conference, IEEE PESC (2000)
12. Silva, J.F.: Electrónica Industrial – Semicondutores e Conversores de Potência. Fundação Calouste Gulbenkian, 2ª edição (2013)